

Research Articles: Behavioral/Cognitive

Holistic recollection via pattern completion involves hippocampal subfield CA3

<https://doi.org/10.1523/JNEUROSCI.0722-19.2019>

Cite as: J. Neurosci 2019; 10.1523/JNEUROSCI.0722-19.2019

Received: 29 March 2019

Revised: 11 July 2019

Accepted: 14 July 2019

This Early Release article has been peer-reviewed and accepted, but has not been through the composition and copyediting processes. The final version may differ slightly in style or formatting and will contain links to any extended data.

Alerts: Sign up at www.jneurosci.org/alerts to receive customized email alerts when the fully formatted version of this article is published.

Copyright © 2019 Grande et al.

This is an open-access article distributed under the terms of the Creative Commons Attribution 4.0 International license, which permits unrestricted use, distribution and reproduction in any medium provided that the original work is properly attributed.

1 Holistic recollection via pattern completion involves hippocampal subfield CA3

2 Running Title: Holistic recollection involves subfield CA3

3 Xenia Grande^{1,2}, David Berron^{1,2,6}, Aidan J. Horner^{7,8}, James A. Bisby^{3,4}, Emrah Düzel*^{1,2,3},

4 Neil Burgess*^{3,4,5}

5 * denotes shared senior authorship

6 (1) German Center for Neurodegenerative Diseases (DZNE), 39120 Magdeburg, Germany

7 (2) Institute of Cognitive Neurology and Dementia Research, Otto-von-Guericke University
8 Magdeburg, 39120 Magdeburg, Germany

9 (3) Institute of Cognitive Neuroscience, University College London, 17 Queen Square, London WC1N
10 3AZ, UK

11 (4) UCL Queen Square Institute of Neurology, University College London, Queen Square, London
12 WC1N 3BG, UK

13 (5) Wellcome Trust Centre for Human Neuroimaging, University College London, 12 Queen Square,
14 London WC1N 3AR, UK

15 (6) Clinical Memory Research Unit, Department of Clinical Sciences Malmö, Lund University, 223 62
16 Lund, Sweden

17 (7) Department of Psychology, University of York YO10 5DD, UK

18 (8) York Biomedical Research Institute, University of York YO10 5DD, UK

19 Corresponding author: Xenia Grande (xenia.grande@dzne.de)

20 Number of pages: 42

21 Number of figures: 7

22 Number of words: 130 (abstract) 603 (introduction) 1488 (discussion)

23 Conflict of interest statement: The authors declare no competing financial interests.

24 Acknowledgements:

25 We thank the Leibniz Institute for Neurobiology in Magdeburg for providing access to the 7 Tesla MR
26 Scanner.

27 This project has received funding from the European Union's Horizon 2020 Research and Innovation
28 Programme under Grant Agreement No. 720270 (HBP SGA1) and Grant Agreement No. 785907 (HBP
29 SGA2). Additional funding was received from the Wellcome Trust (for NB 202805/Z/16/Z and for AJH
30 204277/Z/16/Z). AJH was moreover supported by ESRC (ES/R007454/1).

31 Abstract

32

33 Episodic memories typically comprise multiple elements. A defining characteristic of episodic
34 retrieval is holistic recollection, i.e. comprehensive recall of the elements a memorized event
35 encompasses. A recent study implicated activity in the human hippocampus with holistic recollection
36 of multi-element events based on cues (Horner, Bisby, Bush, Lin, & Burgess et al., 2015). Here, we
37 obtained ultra-high resolution functional neuroimaging data at 7 Tesla in 30 younger adults (12
38 female) using the same paradigm. In accordance with anatomically inspired computational models
39 and animal research, we found that metabolic activity in hippocampal subfield CA3 (but less
40 pronounced in dentate gyrus) correlated with this form of mnemonic pattern completion across
41 participants. Our study provides the first evidence in humans for a strong involvement of
42 hippocampal subfield CA3 in holistic recollection via pattern completion.

43

44 Significance Statement

45

46 Memories of daily events usually involve multiple elements, while a single element can be
47 sufficient to prompt recollection of the whole event. Such holistic recollection is thought to require
48 reactivation of brain activity representing the full event from one event element ('pattern
49 completion'). Computational and animal models suggest that mnemonic pattern completion is
50 accomplished in a specific subregion of the hippocampus called CA3, but empirical evidence in
51 humans was lacking. Here, we leverage the ultra-high resolution of 7 Tesla neuroimaging to provide
52 first evidence for a strong involvement of the human CA3 in holistic recollection of multi-element
53 events via pattern completion.

54

55 Introduction

56

57 Episodic memories bind multiple elements into a single representation. Recollection may be
58 triggered by any one of these elements. Asked, for example, about whether we had been to a certain
59 restaurant before, we may recall meeting a friend there lately. Remarkably, the “restaurant” cue may
60 even initiate *holistic* recollection: Another guest’s dog or the piano in the restaurant may come to our
61 mind. Holistic recollection thus refers to comprehensive recall of the elements an event
62 encompasses, even though incidental to the current situation (Tulving, 1983).

63 Successful pattern completion is considered a prerequisite for such holistic recollection. The
64 cue information needs to be completed towards the full event to produce comprehensive recall
65 (Marr, 1971; McClelland, McNaughton, & O’Reilly, 1995; Treves & Rolls, 1994). A corresponding
66 feature of recollective experiences is the reinstatement of the encoding-related cortical activity
67 (Bosch, Jehee, Fernández, & Doeller, 2014; Gordon, Rissman, Kiani, & Wagner, 2014; Liang & Preston,
68 2017; Staresina, Cooper, & Henson, 2013; Staresina, Henson, Kriegeskorte, & Alink, 2012). Recently,
69 it has been shown that cortical reinstatement of incidentally recalled event elements is related to
70 functional activity in the hippocampus (Horner, Bisby, Bush, Lin, & Burgess, 2015). However, the
71 spatial resolution was not sufficient to dissect the specific involvement of hippocampal subfields.

72 Anatomically inspired computational and theoretical models attribute different information
73 processing mechanisms to different hippocampal subfields. Unique recurrent collaterals in subfield
74 CA3 provide an effective condition for the implementation of pattern completion (Marr, 1971; Treves
75 & Rolls, 1991). Consequently, computational models suggest subfield CA3 to guide the incidental
76 recall of additional event elements based on pattern completion (McClelland et al., 1995; Treves &
77 Rolls, 1994).

78 Empirical support for the functional role of CA3 in pattern completion mainly originates from
79 animal research (Fellini, Florian, Courtney, & Roullet, 2009; Gold & Kesner, 2005; Lee & Kesner, 2004;
80 Nakazawa et al., 2002; Neunuebel & Knierim, 2014; Vazdarjanova & Guzowski, 2004). Until recently

81 the resolution of human functional magnetic resonance imaging (fMRI) did not allow to separate
82 subfield CA3 from dentate gyrus (DG). Therefore, most fMRI studies indiscriminately attribute
83 pattern completion to human subfield CA3/DG (Chen, Olsen, Preston, Glover, & Wagner, 2011;
84 Dudukovic, Preston, Archie, Glover, & Wagner, 2011; Hindy, Ng, & Turk-Browne, 2016; Schapiro,
85 Kustner, & Turk-Browne, 2012). Solely Bonnici et al. (2012) and Chadwick, Bonnici, & Maguire (2014)
86 demonstrated a generalization function selectively in CA3. Evidence for explicit functional
87 engagement of (the human) CA3 in holistic recollection and thus mnemonic pattern completion is
88 still pending.

89 Here, we aimed to provide first empirical evidence at the hippocampal subfield level for the
90 functional underpinnings of holistic recollection via pattern completion in humans using fMRI data
91 with ultra-high resolution at 7 Tesla. We used the same task as Horner and colleagues (2015) during
92 which multi-element events were learned as overlapping pairs of associations between elements
93 (places, people and objects), and subsequently retrieved as paired associations. This task allowed us
94 to assess holistic recollection both behaviorally and in terms of neural activity. That is, we calculated
95 the statistical dependency in performance of retrieving one association from an event on retrieving
96 another association from the same event. We also measured the extent of incidental retrieval of
97 event elements that were neither the cue nor target of retrieval in terms of regional activity during
98 retrieval corresponding to the nontarget element category (e.g. place, people or object). Fully
99 overlapping associations (closed-loops), which appear to create coherent events with holistic
100 recollection, were compared with partially overlapping associations (open-loops), see Horner et al.
101 (2015) for details. We hypothesized that cortical reinstatement of incidental elements during holistic
102 recollection would be associated with activity in hippocampal subfield CA3 but not DG.

103

104 Methods

105

106 Participants

107 In total, 30 participants (12 female, mean (SD) age: 27 (4)) were recruited from the campus of
108 Otto-von-Guericke University Magdeburg and the Leibniz Institute for Neurobiology Magdeburg. All
109 participants reported to be right-handed and without any neurological or psychiatric illness. If
110 necessary, vision was corrected to normal. Minimum educational level of all participants was the
111 German Abitur (A-level). The participants received an allowance of 30 €. The study was approved by
112 the local Ethics Committee of the Otto-von-Guericke University Magdeburg.

113

114 Materials and Procedure

115 Regarding materials and procedure we follow Horner et al.'s, (2015) set up closely. In the
116 following sections the main features of the design are outlined and adjustments that were necessary
117 are specified.

118

119 *Materials*

120 Stimuli consisted of written words that belonged to four categories: locations (e.g. kitchen),
121 objects (e.g. hammer), animals (e.g. mouse) and famous people (e.g. Obama). The words were taken
122 from Horner et al. (2015) and translated into German. To assure a similar level of familiarity within
123 our German sample, several people-stimuli were changed based on preceding behavioral pilot
124 results. In total, 36 events were created by associating one example out of each category with
125 another. Initially, four event sets were built and randomized across participants. For each participant,
126 18 events were assigned randomly to consist of four categories (location – object – people – animal).
127 These events will be referred to as open-loop structure events in the following. The remaining 18
128 events consisted of three categories. Within these closed-loop structure events, 9 events were

129 randomly selected to encompass the categories location – object – people and 9 events to
130 encompass the categories location – animal – people.

131 Words were presented in white font on a black background to the center of a screen (font
132 size = 30) and via a mirror mounted on the head coil, participants could watch the projected screen
133 with a visual angle of $\pm 3^\circ \times \pm 2^\circ$.

134

135 *Task Procedure*

136 Prior to the scanning session, participants received task instructions. The task was described
137 as an associative learning paradigm. They were told to imagine each displayed associative word pair
138 together in one scene as vividly as possible. Importantly, the underlying associative event structure
139 of the stimuli was not revealed and remained implicit.

140 During the scanned encoding phase, participants learned the 36 events in a pair-wise
141 associative manner. The encoding phase consisted of three blocks with 36 trials each, adding up to a
142 total of 108 encoding trials. In each block, one associative pair of each event was presented for 6
143 seconds (e.g. kitchen – hammer out of the event kitchen – hammer – Obama – dog, Figure 1C).

144 Following that procedure, one element within an event overlapped between the first and the second
145 encoding block. At the third block, some events remained as an associative chain and followed an
146 “open-loop” event structure (Figure 1B). Thus, in the last encoding block, the third associative pair
147 from these events overlapped again with one element from previously encoded associates of the
148 respective event (AB – BC – CD). In contrast, “closed-loop” events were structured such that at the
149 last encoding block both elements of the currently encoded associate overlapped with previously
150 encoded elements from the respective event (AB – BC – CA; Figure 1A).

151 The specific category pairing at each block was randomized. However, the third encoding
152 block was restricted to a location – object/animal or a people – object/animal category pair. Further
153 details about the randomization procedure can be found in Horner et al. (2015). No responses were

180 Succeeding the structural data acquisition, two runs of functional data were obtained. Both
181 runs consisted of T2*-weighted echo planar slices (EPI), oriented in parallel to the hippocampal long
182 axis (28 axial slices; TR = 2000 ms; TE = 22ms; matrix size 1536 x 1536; FOV = 256mm x 256 mm;
183 resolution= 0.8 mm, odd-even interleaved slice acquisition). First, functional data regarding the
184 encoding phase was obtained (440 volumes). Second, the functional data regarding the retrieval
185 phase was obtained (approximately 700 volumes, depending on response times). Responses were
186 recorded using a scanner-compatible 4-choice button box. The complete scanning procedure took
187 approximately 80 min.

188 The functional data was distortion corrected by means of a point spread function (Zaitsev,
189 Hennig, & Speck, 2004) and online motion corrected during image reconstruction.

190

191 Behavioral Data Analyses

192 The overall accuracy per participant was calculated as the percentage of correct retrieval
193 trials. Note that there are 6 retrieval trials for each of the 36 events. We calculated accuracy
194 separately for closed- and open-loop events. With a paired samples t-test, we tested for significant
195 differences in performance between loop conditions (closed- versus open-loop events). We also
196 evaluated the amount of retrieval dependency among the elements within an event, separately for
197 closed- and open-loop events. This measure reflects the likelihood that an element is successfully
198 retrieved, given successful retrieval of the other elements that belong to the same event. The
199 dependency measures were calculated by means of participant-specific contingency tables. In total,
200 six contingency table were created per participant, one for each category (location (A), people (B),
201 object (C)) being either cue or target. The cue-based tables reflect the retrieval dependency of two
202 elements from the same event across separate retrieval trials, given the trials used the same cue
203 element from the respective event (AbAc). The target-based tables reflect the retrieval dependency
204 of the same target element across separate retrieval trials, given the trials used different cue
205 elements belonging to the same event (BaCa). Each table's cells contain the retrieval performance

206 across events for the respective condition. The dependency measure based on observed data is
207 defined as the proportion of events for which both overlapping associations related to a common
208 element (either being cue or target) are retrieved successfully or unsuccessfully.

209 To assess the dependency measures from the data, we compared them with both a model
210 that assumes full retrieval dependency, and a model that assumes full retrieval independency among
211 all elements of an event. The expected dependency based on the independent model was estimated
212 by multiplying the probabilities of separately retrieving either of the two items of an event within the
213 contingency tables. The dependent model is based on the independent model but estimates the
214 expected dependency by accounting for the level of guessing and inserting an “episodic factor”. This
215 “episodic factor” weights the performance for a certain event by a factor that captures the difference
216 between the respective event’s performance across separate retrieval trials versus general
217 performance across all events. Note, that the measure of observed dependency scales with accuracy.
218 Therefore, only comparisons between observed dependency measures and model-based expected
219 dependency values are informative. Comparisons between dependency measures were made using
220 paired-samples t-tests for both event structure conditions (open-loop and closed-loop), separately.
221 For further details on the calculation of dependency measures based on the data and based on the
222 two models, see Horner et al. (2015) and Horner & Burgess (2013).

223 To gain an impression of dependency differences that might be masked due to high accuracy
224 levels in both loop conditions (88.55% and 86.27% for closed- and open-loop, respectively), the
225 confidence level was taken into account. Dependency measures were evaluated in the above
226 described manner. However, instead of calculating dependency measures based on contingency
227 tables that refer to correct versus incorrect retrieval, now the contingency tables were refined to
228 reflect high confidence (score 4 or 3) versus low confidence (score 1 or 2) or incorrect retrieval.
229 Statistical comparisons between dependency scores in different event loop conditions were made
230 with paired-samples t-test. As indicated above, these comparisons involve the differences in

231 observed dependency and expected dependency based on the independent model in respective
232 conditions.

233

234 Functional Data Analyses

235 *Preprocessing*

236 All preprocessing steps were performed with SPM12 (Statistical Parametric Mapping, Version
237 12, Wellcome Trust Centre for Neuroimaging, University College London; RRID:SCR_007037; Penny,
238 Friston, Ashburner, Kiebel, & Nichols, 2011). The raw functional data was distortion and motion
239 corrected already (see fMRI acquisition). First, the raw data was converted from DICOM into Nifti
240 format. Second, slice timing correction was applied and the data was smoothed with a full-width
241 half-maximum Gaussian kernel of 2x2x2 mm. The size of the kernel was chosen based on previous
242 reports to preserve high specificity but increase sensitivity at the same time (Berron et al., 2016;
243 Maass, Berron, Libby, Ranganath, & Düzel, 2015).

244 Outliers based on motion (threshold 2 mm) or global signal (threshold 9.0) were detected by
245 the ARTifact detection Tools (ART) software package (RRID:SCR_005994; Mozes & Whitfield-Gabrieli,
246 2011). The fully preprocessed data was used for outlier detection. The procedure resulted in a vector
247 for each participant that indicated outlier scans. They were entered as separate regressors into all
248 univariate analyses (see below).

249

250 *Structural template calculation (T1 weighted)*

251 To calculate and visualize functional analyses results on group level, a sample-specific
252 template was created for the T1-weighted structural volumes. This assures optimal alignment of the
253 functional data across participant (Avants et al., 2011). We used the nonlinear diffeomorphic
254 mapping procedure called “buildtemplateparallel.sh” provided by Advanced Normalization Tools
255 (ANTS) to construct a T1-template based on the 30 whole-brain T1-weighted volumes obtained from
256 all participants (RRID:SCR_004757; Avants et al., 2010).

257

258

259 *Hippocampal segmentation*

260 The current study aimed to examine specific functional activity patterns in the hippocampus.

261 Thus, we restricted several functional analyses (indicated below) to hippocampal regions of interest

262 (ROI). Using ITK-SNAP (RRID:SCR_002010; Yushkevich et al., 2006) we manually segmented the

263 bilateral hippocampus in all 30 participants on their specific T2-weighted structural volume. Therein

264 we followed the segmentation protocol by Berron et al. (2017). This yielded participant-specific

265 masks for HC subfields CA1, CA2, CA3, Subiculum and DG, one for each hemisphere.

266 To use these masks as anatomical regions of interests in the functional analyses, each

267 participant-specific T2-weighted HC subfield mask was coregistered to the participant's EPI-space

268 and resampled to the EPI-resolution. This was accomplished in two steps. First, SPM12 was used to

269 coregister and resample the T2-weighted HC subfields masks to the individual T1 space by applying

270 "spm_coreg" (Penny et al., 2011). Second, these masks were coregistered from the individual T1

271 space to the EPI space using FSL FLIRT (RRID:SCR_002823; Greve & Fischl, 2009; Jenkinson, Bannister,

272 Brady, & Smith, 2002; Jenkinson & Smith, 2001). See Figure 2 for an example segmentation and

273 coregistration from T2 to EPI space.

274 All masks were divided in an anterior and a posterior part. To that end, the main

275 hippocampal extension in each hemisphere was defined for each individual by taking the outer parts

276 of the z-dimension. All hippocampal subfields of that participant within that hemisphere were split in

277 two at the border identified by half the length of the total hippocampus in z direction.

278

--- Figure 2 ---

279

280

281

282

283 *General functional analyses approach*

284 All functional analyses were performed with SPM12 (Statistical Parametric Mapping, Version
285 12, Wellcome Trust Centre for Neuroimaging, University College London; Penny et al., 2011)) on
286 single participant and group level.

287 *Functional analysis at the participant level.* At the first level, a general linear model was fit to
288 each participant's functional data in native space. Therefore, the underlying neural data was
289 modelled by a boxcar function at stimulus onset for each condition of interest (dependent on the
290 respective analysis). The resulting neural model was convolved by a canonical hemodynamic
291 response function to predict the functional data. Besides the regressors predicting the functional
292 data related to each condition of interest, each general linear model also included one intercept
293 regressor and six motion correction parameters as regressor of no interest. The motion-correction
294 parameters were added to capture variability related to task-correlated motion and reduce the
295 amount of false-positive activity in task conditions (Johnstone et al., 2006). If applicable, a regressor
296 of no interest was added to capture variance in the functional data related to the outlier scans. Each
297 general linear model was fit to the acquired functional data to obtain parameter estimates for each
298 condition of interest. To examine differences in BOLD activity related to the conditions of interest,
299 contrast maps were calculated for each participant in native space (specific contrasts dependent on
300 respective analysis).

301 *Normalization.* To be able to assess consistent contrast effects at group level, we normalized
302 each participant's contrast maps to the group T1 template. Therefore, we first normalized each
303 participant's mean functional echo-planar image to the participant's structural T1 image and then to
304 the T1 group template by using FSL "epi_reg" (Greve & Fischl, 2009; Jenkinson et al., 2002; Jenkinson
305 & Smith, 2001) and ANTS "WarpImageMultiTransform.sh" respectively (Avants et al., 2010, 2011).
306 This procedure resulted in participant-specific transformation matrices that could then be used for
307 the spatial normalization of the contrast maps.

308 *Second level group analyses.* For group analyses, we assessed consistent differences in
309 functional activity across participants. Therefore, the spatially normalized contrast maps from each
310 participant were entered into a general linear model using SPM12 (Penny et al., 2011). Unless stated
311 otherwise, group results are reported with an initial cluster defining threshold of $p < .005$.

312

313 Functional analyses in detail

314 Two participants were excluded from all functional analyses due to an amount of outlier
315 scans exceeding 10 % of the total scans at retrieval. Outliers were determined by excessive motion
316 (threshold 2 mm) or global signal changes (threshold 9.0). In addition, all region-of-interest analyses
317 within hippocampal subfields were conducted with one participant less due to motion in the T2
318 image of that participant which made hippocampal subfield segmentation impossible.

319 For all analyses the object and animal conditions were merged (see Horner et al., 2015).
320 Note, that we did not see any specific functional activity for animals in the ‘retrieval phase – element
321 specific activity’ analysis (see below). When lowering the threshold ($p < .005$, uncorrected), however,
322 functional clusters were comparable to the object condition (in lateral occipital cortex). As we did not
323 see differences in functional activity, we collapsed object and animal conditions to assure
324 comparability of results with Horner et al. (2015). The animal and the object condition will both be
325 referred to as the object category in the following.

326

327 *Retrieval phase – element specific activity*

328 To examine significant clusters of functional activity related to specific categories of event
329 elements, we set up a general linear model with 7 regressors of interest. Each regressor included the
330 boxcar convolved stimulus onsets for one type of cue-target association (location – object; object –
331 location; object – people; people – object; people – location; location – people). Each trial duration
332 was determined by the response time. An additional regressor was included that modelled the
333 interstimulus interval with a duration of 1.5 seconds. To assess differences in functional activity

334 related to the three element categories, contrast maps were obtained between the parameter
335 estimates related to the regressors that contained the respective category and those that did not
336 contain the respective category. For instance, to obtain location related clusters of significant
337 functional activity, we contrasted the parameter estimates obtained for the location-object, object-
338 location, location-people and people-location regressors with the parameter estimates for the
339 object-people and people-object regressors.

340 To examine consistent clusters of significant functional activity at group level, the normalized
341 contrast maps were entered into a one sample t-test on second level. All results are reported with
342 family-wise error correction after applying an initial cluster defining threshold of $p < .001$.

343

344

345 *Cortical reinstatement at retrieval*

346 Here, we initially evaluated whether the function an element occupies at retrieval (cue,
347 target or nontarget) entails differences in the overall amount of cortical reinstatement.
348 Subsequently, differences in cortical reinstatement of cues, targets and nontargets between closed-
349 and open-loop events were explored.

350 To begin with, the amount of cortical reinstatement was assessed for each function an
351 element could take (cue, target and nontarget), across event loop conditions. This yielded an overall
352 cortical reinstatement score per element function and participant (Figure 3A). Based on the previous
353 analysis (retrieval phase - element specific activity) we obtained a significant cortical functional
354 cluster for each category (location, people and object) at the group level (Figure 3A(ii)). In the case of
355 multiple significant functional clusters, we focused on the element-specific ROI that was identified by
356 Horner et al. (2015) to assure comparability of results (note that we obtained comparable results
357 when using all our identified clusters). The corresponding functional masks were coregistered to each
358 participant's native space with FSL FLIRT (Greve & Fischl, 2009; Jenkinson et al., 2002; Jenkinson &
359 Smith, 2001). Using REX (RRID:SCR_005994; Whitfield-Gabrieli, 2009), we then extracted participant-

360 specific parameter estimates for each regressor of interest in the element specific activity analysis
361 out of each element-specific ROI. Parameter estimates within each ROI were z-standardized. To
362 obtain a participant specific value for the amount of cortical reinstatement related to each element
363 function, we took the parameter estimates out of each ROI, first for the condition that the respective
364 ROI was related to the category of the cue (“cue cortical reinstatement”), second for the condition
365 that the respective ROI was related to the category of the target (“target cortical reinstatement”),
366 and third for the condition that the respective ROI was neither related to the category of the cue or
367 the target but only related to the nontarget category (“nontarget cortical reinstatement”, Figure 3A).
368 For instance, the previous analysis (element-specific activity at retrieval) found a significant cluster of
369 increased functional activity in the parahippocampal cortex for location category stimuli. Now, we
370 took the parameter estimate regarding the people-object and object-people condition out of the
371 parahippocampal cortex to obtain a measure for the nontarget cortical reinstatement for when the
372 location was nontarget. Similarly we proceeded for the remaining two categories (people, object) to
373 obtain nontarget cortical reinstatement values for each category. The normalized parameter
374 estimates were averaged across ROIs (i.e. categories) for each participant, separately for cue, target
375 and nontarget cortical reinstatement (Figure 3A(iii)). Differences in the amount of overall cortical
376 reinstatement between element functions (cue, target, nontarget) were tested using a repeated
377 measures ANOVA.

378 To further explore the differences in cortical reinstatement between closed- and open-loop
379 events, we then evaluated cortical functional activity for both event loop conditions. To compare
380 cortical reinstatement between event loop conditions, we had to delineate functional cortical activity
381 for closed- and open-loop events. Therefore, the above described univariate analysis (element-
382 specific activity at retrieval) was performed again. Instead of 7 regressors of interest, 14 were
383 created, they contained the same information as the 7 in the analysis before, now split up into trials
384 that belonged to closed-loop and open-loop events. Then, the same procedure was followed as
385 described above to acquire element-related cortical activity values for cue, target and nontargets per

386 participant. Now however, calculated for closed-loop events and open-loop events separately.
387 Subsequently, obtained difference scores for cortical reinstatement between event loop conditions
388 were tested for significant deviation from zero by using one-sample t-tests to assess whether cortical
389 reinstatement was higher in closed-loop events.

390

391 *Hippocampal activity and cortical reinstatement*

392 The following analyses were aimed to identify activity clusters in the hippocampus that
393 functionally relate to holistic recollection and to delineate their subfield-specific localization. As
394 holistic recollection is conceptualized to be measurable by the amount of nontarget cortical
395 reinstatement, we assessed hippocampal functional correlates of increased nontarget cortical
396 reinstatement in closed-loop events.

397 We first followed an exploratory parametric analysis approach to assess whether any
398 hippocampal cluster correlates with nontarget cortical reinstatement under conditions of increased
399 holistic recollection. Therefore, initially a univariate first level analysis was performed. The general
400 linear model encompassed three regressors of interest. One contained the boxcar function
401 convolved stimulus onsets for trials that are part of closed-loop events (duration equaled response
402 time). The second regressor contained the boxcar function convolved stimulus onsets for trials that
403 belong to open-loop events (duration equaled response time). The third regressor contained the
404 boxcar convolved onsets of the inter stimulus intervals (duration 1.5 seconds). Contrast maps were
405 obtained for each participant for closed-loop versus open-loop event retrieval trials.

406 To investigate hippocampal involvement in holistic recollection, that is particularly the
407 cortical reinstatement of nontargets, we used the first level contrast maps that indicated for each
408 individual where in the hippocampus BOLD activity was greater for closed-loop than open-loop event
409 retrieval (Figure 3B). With the second level group analysis, we investigated which of the functional
410 activity clusters that related to closed-loop retrieval correlate with the amount of nontarget cortical
411 reinstatement across participants (Figure 3B). To assess the functional specificity of the revealed

412 significant cluster at nontarget cortical reinstatement, the second level group analysis was performed
413 two more times, additionally for cue cortical reinstatement and target cortical reinstatement. Each
414 general linear model included the normalized contrast maps for the contrast closed > open-loop
415 retrieval of each participant as a first regressor. The second regressor included the respective
416 participant-specific value for cue, target or nontarget reinstatement, obtained by the independent
417 analysis of element-category related cortical activity at retrieval (Figure 32A). All results are reported
418 with an initial cluster defining threshold of $p < .005$. Small volume correction with a bilateral
419 hippocampal mask was applied at second level.

420 To assess whether the identified hippocampal cluster correlated more with nontarget cortical
421 reinstatement than with cue or target reinstatement, participant-specific mean functional activity
422 was extracted from the respective cluster for the contrast closed > open-loop retrieval with REX
423 (Whitfield-Gabrieli, 2009). Pearson correlation coefficients for each cortical reinstatement type (cue,
424 target and nontarget) with the extracted functional cluster activity were obtained. With a one-tailed
425 z-test we tested whether the obtained Pearson correlation coefficients were significantly higher for
426 nontarget reinstatement than for cue and target reinstatement respectively (Diedenhofen & Musch,
427 2015; Rosenthal, Rubin, & Meng, 1992).

428 The clusters identified by above described analyses can only be attributed to a specific
429 subfield by visual inspection. As they were considered to be located close to the right anterior CA3-
430 DG border, a subsequent region-of-interest analysis was performed to delineate functional
431 involvement of CA3 versus DG. Therefore, mean beta values from the first level analyses were
432 extracted using REX (Whitfield-Gabrieli, 2009) for each individual out of the manually segmented
433 hippocampal subfields masks for right anterior CA3 and right anterior DG. Beta values were extracted
434 referring to the closed-loop regressor and to the open-loop regressor. Pearson correlation
435 coefficients and corresponding significance values were obtained for the relationship between the
436 difference in beta values (closed- versus open-loop) and the amount of nontarget reinstatement
437 across participants. With a one-tailed z-test we tested whether the obtained Pearson correlation

Holistic recollection involves subfield CA3

438 coefficient was significantly higher for right anterior CA3 than right anterior DG (Diedenhofen &
439 Musch, 2015; Rosenthal et al., 1992).

440 --- *Figure 3* ---

441

442 Results

443

444 Behavioral Results

445 On average 87.41% (SD = 9.78%) of all trials in the recall phase were answered correctly by
446 the 30 participants. There was no significant difference in accuracy between closed-loop (mean =
447 88.55%, SD = 8.96%) and open-loop events (mean = 86.27%, SD = 10.60%).

448 We also investigated the amount of dependency among event elements. Note, that the
449 dependency measure we calculated scales with accuracy. Therefore the evidence for dependency is
450 defined as the difference between data-based dependency and the expected dependency based on
451 the independent model. The evidence for dependency is not significantly higher for closed- than
452 open-loop events ($t(29) = 1.162$; $p = .255$). The higher the overall accuracy, the more dependency
453 values approach 1 (also see Horner et al., 2015). Our very high accuracy may thus have led to ceiling
454 levels in the estimated dependency measures, making it impossible to detect differences between
455 open- and closed-loop event dependency.

456 To test whether the high overall accuracy may have obscured stronger dependency among
457 closed-loop elements, we calculated dependency again by taking the confidence level into account.
458 That is, instead of classifying the retrieval trials by correct versus incorrect, we split them into high
459 and low confidence trials and collapsed incorrect and low confidence trials. The evidence for
460 dependency is not significantly different between loop conditions ($t(29) = 1.978$; $p = .058$). However,
461 open-loop events but not closed-loop events showed significantly lower dependency than the
462 dependent model ($t(29) = -2.59$; $p = .015$ and $t(29) = -1.47$; $p = .152$). Numerically, our results are
463 consistent with previous results (Horner et al., 2014; Horner et al., 2015). That is, retrieval at closed-
464 loop events entails more dependency among event elements than retrieval at open-loop events
465 (Figure 4).

466

--- Figure 4 ---

467

468 Univariate Results

469 *Element-specific cortical activity at retrieval*

470 The aim of this analysis was to identify element-specific cortical functional activity patterns at
471 retrieval. Therefore, category associations that contained a respective element were contrasted with
472 category associations that did not contain the respective element (e.g. identify location activity by
473 contrasting location – object and location – people with people – object trials).

474 People-related activity was found in the medial parietal lobe (cluster size $k = 1172$, $p < .001$,
475 see Figure 3A(i)), in a left inferior temporal cluster (cluster size $k = 103$, $p = .006$) and in a right lateral
476 parietal cluster (cluster size $k = 126$, $p = .001$). Object-related activity was found in the left lateral
477 occipital lobe (separated into three clusters, first cluster size $k = 864$, $p < .001$, see Figure 3A(i);
478 second cluster size $k = 101$, $p = .006$, third cluster size $k = 75$, $p = .041$). Location-related activity was
479 found in bilateral clusters in the parahippocampal cortex (left cluster size $k = 2242$, $p < .001$, right
480 cluster size $k = 883$, $p < .001$, see Figure 3A(i)), bilateral retrosplenial cortex (cluster size $k = 7786$, $p <$
481 $.001$) and bilateral lateral parietal cortex (left cluster size $k = 698$, $p < .001$, right cluster size $k = 418$, p
482 $< .001$).

483

484 *Cortical reinstatement during closed-loop event retrieval*

485 The identification of element-specific activity patterns at retrieval allowed us to obtain
486 participant-specific values for the amount of cortical reinstatement at retrieval (Figure 3A).
487 Therefore, parameter estimates were extracted from each element-specific cortical region when the
488 respective element functioned as a cue, target or nontarget. We averaged these values across
489 element categories. Note that, when multiple element-specific clusters have been identified, we
490 extracted parameter estimates exclusively from the region selected by Horner et al. (2015) to assure
491 comparability of results (i.e. people: medial parietal cluster, animal/object: left lateral occipital
492 cluster, location: bilateral parahippocampal cluster). Thus, we obtained three values per participant
493 that reflect the element-related cortical activity at retrieval: First, the cue cortical reinstatement,

494 thus the functional cortical activity induced by cues, second, the target cortical reinstatement, that is
495 functional cortical activity induced by targets and third, the cortical reinstatement of nontargets, i.e.
496 the cortical reinstatement of event elements currently incidental to the task.

497 Over all experimental conditions, cue and target cortical reinstatement was significantly
498 higher than nontarget cortical reinstatement, and targets induced significantly more cortical activity
499 than cue elements (Figure 5A; main effect of element function $F(2,75) = 111.35$; $p < .001$, ANOVA).
500 Note that the displayed beta values are not in relationship to an explicit baseline but rather the
501 overall mean parameter estimate. Differences are thus not absolute but relative to each other. We
502 operationalized holistic recollection as the amount of incidental reinstatement, i.e. reactivation
503 corresponding to nontarget elements. To test whether closed-loop event retrieval entails more
504 holistic recollection, we investigated whether more nontarget cortical reinstatement took place for
505 closed-loop than open-loop event retrieval (see Figure 3B). Indeed, the difference between the
506 amount of element-related cortical activity in closed- and open-loop conditions is only significantly
507 higher than zero for nontargets ($t(25) = 2.46$, $p = .02$), not so for cues ($t(25) = -1.04$, $p > .05$) or targets
508 ($t(25) = -.05$, $p > .05$; Figure 5B; one-sample t-tests). Thus, cortical reinstatement of nontargets was
509 higher for closed-loop than open-loop retrieval.

510 --- Figure 5 ---

511

512 *Anterior CA3, but not DG activity during closed-loop retrieval correlates with overall nontarget*
513 *reinstatement*

514 Phenomenological differences between closed- and open-loop retrieval in terms of holistic
515 recollection, i.e. the amount of nontarget cortical reinstatement, are apparent based on the previous
516 analyses. We therefore examined whether there are specific hippocampal functional correlates of
517 closed-loop event retrieval. When functional differences between closed- and open-loop event
518 retrieval are related to holistic recollection, they should scale with the amount of nontarget
519 reinstatement a participant engages in.

520 First, we contrasted BOLD activity during closed- and open-loop event retrieval within each
521 participant. This yielded participant-specific statistical maps indicating functional activity differences
522 between both loop structures. At the group level these contrast maps were then correlated with the
523 participant-specific amount of nontarget cortical reinstatement. This explorative approach yields
524 clusters within the hippocampus that display increased functional involvement during closed-loop
525 event retrieval when overall nontarget cortical reinstatement, i.e. holistic recollection, is high (Figure
526 3B). An anterior right hippocampal cluster (cluster size $k = 35$; $p(\text{cluster}) = .028$ (uncorr)), located in
527 subfield CA3, was revealed that scales its functional activity during closed-loop event retrieval with
528 the participant's amount of overall nontarget cortical reinstatement (Figure 6A). Note, that no
529 significant clusters could be identified for the reverse correlation and when correlating individual
530 contrast maps for open > closed-loop retrieval with the overall nontarget cortical reinstatement
531 across individuals.

532 To test whether the identified cluster was specific for nontarget reinstatement, i.e. holistic
533 recollection, and not related to other retrieval processes, we first tested whether the respective
534 cluster correlated with cue and target reinstatement as well. Pearson correlations between cluster
535 activity (i.e. extracted beta values for the closed – open-loop contrast) and cue as well as target
536 reinstatement were significantly lower than the previously identified correlation of the right anterior
537 CA3 cluster with nontarget reinstatement ($z = -2.584$, $p = .005$ and $z = -3.226$, $p = .001$ for the
538 difference in correlations between $p(\text{nontarget reinstatement, cluster activity})$ and $p(\text{cue}$
539 $\text{reinstatement, cluster activity})$ or $p(\text{target reinstatement, cluster activity})$, respectively). Second, we
540 investigated whether additional anterior hippocampal activity is related to cue or target induced
541 cortical activity. Therefore, the same parametric analyses approach was adopted at group level as we
542 applied for the identification of hippocampal activity related to nontarget reinstatement. Now,
543 however we correlated the difference in functional activity between loop conditions with cue and
544 target cortical reinstatement respectively. No anterior hippocampal cluster showed increased

567 Discussion

568

569 Using ultra-high resolution 7 Tesla fMRI, we provide first empirical evidence for the
570 involvement of human hippocampal subfield CA3 in holistic recollection via pattern completion.
571 Therein we go beyond a replication of the main findings by Horner et al. (2015) and unpack the
572 functional involvement of hippocampal subfields at recollection of multi-element events.

573 Our paradigm relies upon the assumption that multi-element events composed as a closed-
574 loop entail more holistic recollection at retrieval than events with an open-loop structure. Extensive
575 previous research provides support for an increased dependency among event elements that are
576 encoded in an all-to-all associative manner (Horner et al., 2015; Horner & Burgess, 2013, 2014). The
577 likelihood to incidentally retrieve event elements when cued with one element, i.e. for holistic
578 recollection is therefore increased in closed-loop events. Consequently, cortical reinstatement of
579 incidental event elements has been shown and here again been confirmed to be higher when
580 retrieving closed-loop events (Horner et al., 2015; Figure 4 and 5). We additionally demonstrated
581 increased functional involvement of right anterior subfield CA3 at closed-loop event retrieval in
582 relation to cortical reinstatement of incidental elements (Figure 6A). Our data indicate that anterior
583 CA3 activity is related to successful pattern completion associated with holistic recollection. Thereby
584 we contribute to recent efforts in empirically addressing the functional subfield architecture of the
585 human hippocampus.

586 While models of the functional organization of hippocampal subfields (Amaral & Witter,
587 1989; Hunsaker & Kesner, 2013; Lisman, 1999) have been informed by anatomical and animal
588 research, the translation of these insights to humans has been limited by the resolution of fMRI,
589 particularly in distinguishing functional activity in CA3 and DG. Here, we were able to acquire
590 functional images with a submillimeter resolution (0.8 mm isotropic) allowing us to segment CA3 and
591 DG separately and to examine specific functional patterns of both subfields (Berron et al., 2016).
592 Indeed, the anatomical ROI analysis confirms that the association between functional subfield

593 activity and the amount of holistic recollection particularly holds for anterior CA3 but less for the
594 adjacent DG (Figure 7). The association between subfield CA3 and a condition that entails more
595 pattern completion is in accordance with previous animal research (Fellini et al., 2009; Gold &
596 Kesner, 2005; Lee & Kesner, 2004; Nakazawa et al., 2002; Neunuebel & Knierim, 2014; Vazdarjanova
597 & Guzowski, 2004).

598 Despite proposed anatomical and functional heterogeneity between hippocampal subfields,
599 recent human functional imaging showed functional heterogeneity along the longitudinal axis (e.g.
600 Brunec et al., 2018; Collin, Milivojevic, & Doeller, 2015). Interestingly, proposals exist for scene
601 imagination, transitive inference processes and pattern completion being related to the anterior
602 hippocampus (Poppenk, Evensmoen, Moscovitch, & Nadel, 2013; Strange, Witter, Lein, & Moser,
603 2014; Zeidman & Maguire, 2016). Our finding of anterior hippocampal involvement in holistic
604 recollection might be seen in line with that literature.

605 Also along the transversal axis of the hippocampus considerable heterogeneity has been
606 suggested. Importantly, the anatomical transition between subfields is not decisive but rather graded
607 (Amaral & Witter, 1989). This renders it difficult to strictly examine functional activity of CA3 and DG
608 independently. Moreover, despite the usage of ultra-high resolution functional imaging, 2 mm
609 smoothing was applied which blurs functional data at the border of segmented subfields.
610 Nevertheless, our anatomical ROI analysis averages functional signal across whole subfields that
611 extend more than the 2 mm smoothing radius. The observed significant correlation between CA3
612 activity and holistic recollection is thus, even though not completely independent from DG activity, a
613 confirmation of CA3 being significantly involved at successful holistic recollection.

614 Particularly in the anterior medial part (i.e. uncus region), hippocampal anatomy is highly
615 complex and variable between individuals (Ding & Van Hoesen, 2015). Therefore, some subfield
616 segmentation protocols decided to spare this region (e.g. Dalton, Zeidman, Barry, Williams, &
617 Maguire, 2017). Indeed, subfield specific interpretations in the hippocampal head should be drawn
618 with caution. However, the segmentation protocol, that we have applied, leveraged the higher

619 resolution at 7T (i.e. 1 mm slice thickness) to translate recent findings on subfield boundaries in the
620 hippocampal head from neuroanatomy to MRI (Ding & Van Hoesen, 2015; Berron et al., 2017).

621 Note, that the cortical reinstatement of incidental elements (“nontargets”, Figure 3) is an
622 indirect measure for hippocampal pattern completion. Theoretical models propose that successful
623 retrieval is initiated by completing a cue pattern towards the full event representation in the
624 hippocampus (Marr, 1971; McClelland, 1995; Treves & Rolls, 1994). Pattern completion may go
625 beyond the required target and include nontargets, particularly if the event representation binds
626 multiple elements tightly together (as e.g. in closed-loop events, Horner et al., 2015; Horner &
627 Burgess, 2014). The elements of the completed event representation are subsequently reinstated in
628 the cortex, which then creates a recollective experience (Bosch et al., 2014; Gordon et al., 2014;
629 Liang & Preston, 2017; Staresina et al., 2012; Staresina, Cooper, & Henson, 2013; Thakral, Wang, &
630 Rugg, 2015). Thus, our observation of increased cortical activity associated with incidental event
631 elements upon retrieval, and its correlation with activity in CA3 supports these models and implicates
632 CA3 in hippocampal pattern completion and holistic recollection.

633 Even though our measure of pattern completion is indirect, several aspects of our results
634 support the specific involvement of anterior CA3 in holistic recollection. First, the anterior CA3
635 cluster related to cortical reinstatement of nontargets could not be identified in relationship to cue
636 or target cortical activity and functional activity within the CA3 cluster was not correlated with
637 reinstatement of cues or targets (Figure 6B). As cues and targets are presented on screen, successful
638 pattern completion is less relevant for the retrieval of these elements. The increased activity of
639 anterior CA3 at closed-loop event recollection when nontarget cortical reinstatement is high, can
640 thus be referred back to the increased engagement of a pattern completion mechanism (Horner et
641 al., 2015). Second, the anterior CA3 involvement at closed-loop event retrieval cannot be explained
642 by mere recall success. Despite more holistic recollection at closed-loop events (i.e. higher retrieval
643 dependency and more nontarget reinstatement), accuracy levels in both event structure conditions
644 are similar. This rules out performance to be a driving factor in the functional activity pattern of

645 anterior CA3. Importantly, we observed CA3 activity in relation to the amount of holistic recollection
646 during the whole task, averaged across both event loop conditions (i.e. in relation to *overall* holistic
647 recollection). Thus, participants that generally engaged in more holistic recollection, showed more
648 CA3 activity when retrieving closed-loop events. In contrast, Horner and colleagues (2015) observed
649 that hippocampal involvement at retrieval of closed-loop events increased with the *difference* in
650 holistic recollection between closed and open-loop events. Small variations in our data may explain
651 the subtle differences in results. Even though we similarly observed higher nontarget reinstatement
652 at retrieval of closed-loop events (Figure 5), the difference to nontarget reinstatement at open-loop
653 events was smaller than in Horner et al. (2015). In our data, performance in both loop conditions was
654 higher and there was more holistic recollection in open-loop events (Figure 4; perhaps due to higher
655 performing participants inferring the missing associations), so that differences between closed- and
656 open-loop events were reduced.

657 While we leveraged the closed- versus open-loop contrast to examine specific hippocampal
658 involvement during holistic recollection via pattern completion, we do not claim that the
659 hippocampus is not involved in the recollection of open-loop associations. The hippocampus likely
660 mediates the associative memory required to answer the paired-associate questions regarding both
661 open- and closed-loop events. However, the open-loop events serve as a strict control condition, as
662 our data and previous literature indicate that there will be greater pattern completion for closed-
663 loop events, resulting in tighter dependency among elements and greater incidental reactivation of
664 nontarget elements (Horner et al., 2015; Horner & Burgess, 2014). Pattern completion is defined as a
665 computational mechanism on representational level (McClelland et al., 1995; Treves & Rolls, 1994).
666 We, however, took a univariate analysis approach here. Moreover, as we averaged across trials and
667 restricted our cortical reinstatement analysis to ROIs, we may not have captured the full variety in
668 the functional activity pattern at holistic recollection. Future studies need to verify pattern
669 completion mechanisms in the human CA3 on trial-specific level as well as directly on
670 representational level by multivariate approaches. The hippocampal effects need to be related to

671 cortical reinstatement beyond our restricted ROIs. In addition, future ultra-high resolution
672 neuroimaging studies should dissect the potential heterogeneity in the functional architecture along
673 the hippocampal axes. Such spatially and temporally more fine-grained analyses will have the
674 potential to show pattern completion effects in the human brain more explicitly.

675 To sum up, we acquired functional data in ultra-high resolution with 7 Tesla fMRI using the
676 established multi-element event paradigm by Horner and colleagues (2015). In accordance with
677 anatomical and animal research, our results yield first compelling empirical evidence for a functional
678 involvement of the human hippocampal subfield CA3 (but less pronounced in DG) in holistic
679 recollection via pattern completion. The current study contributes to our understanding of the
680 heterogeneous functional architecture within the human hippocampus.

681

682 References

683

684 Amaral, D. G., & Witter, M. P. (1989). The three-dimensional organization of the hippocampal
685 formation: A review of anatomical data. *Neuroscience*, *31*(3), 571–591.

686 [https://doi.org/10.1016/0306-4522\(89\)90424-7](https://doi.org/10.1016/0306-4522(89)90424-7)

687 Avants, B. B., Tustison, N. J., Song, G., Cook, P. A., Klein, A., & Gee, J. C. (2011). A reproducible
688 evaluation of ANTs similarity metric performance in brain image registration. *NeuroImage*,
689 *54*(3), 2033–44. <https://doi.org/10.1016/j.neuroimage.2010.09.025>

690 Avants, B. B., Yushkevich, P., Pluta, J., Minkoff, D., Korczykowski, M., Detre, J., & Gee, J. C. (2010). The
691 optimal template effect in hippocampus studies of diseased populations. *NeuroImage*.

692 <https://doi.org/10.1016/j.neuroimage.2009.09.062>

693 Berron, D., Schütze, H., Maass, A., Cardenas-Blanco, A., Kuijf, H. J., Kumaran, D., & Düzel, E. (2016).

694 Strong Evidence for Pattern Separation in Human Dentate Gyrus. *The Journal of Neuroscience :
695 The Official Journal of the Society for Neuroscience*, *36*(29), 7569–79.

696 <https://doi.org/10.1523/JNEUROSCI.0518-16.2016>

697 Berron, D., Vieweg, P., Hochkepler, A., Pluta, J. B., Ding, S. L., Maass, A., ... Wisse, L. E. M. (2017). A
698 protocol for manual segmentation of medial temporal lobe subregions in 7 Tesla MRI.

699 *NeuroImage: Clinical*, *15*, 466–482. <https://doi.org/10.1016/j.nicl.2017.05.022>

700 Bonnici, H. M., Chadwick, M. J., Kumaran, D., Hassabis, D., Weiskopf, N., & Maguire, E. A. (2012).

701 Multi-voxel pattern analysis in human hippocampal subfields. *Frontiers in Human Neuroscience*,
702 *6*, 290. <https://doi.org/10.3389/fnhum.2012.00290>

703 Bosch, S. E., Jehee, J. F. M., Fernández, G., & Doeller, C. F. (2014). Reinstatement of associative

704 memories in early visual cortex is signaled by the hippocampus. *The Journal of Neuroscience :
705 The Official Journal of the Society for Neuroscience*, *34*(22), 7493–500.

706 <https://doi.org/10.1523/JNEUROSCI.0805-14.2014>

707 Brunec, I. K., Bellana, B., Ozubko, J. D., Man, V., Robin, J., Liu, Z.-X., ... Moscovitch, M. (2018). Multiple

- 708 Scales of Representation along the Hippocampal Anteroposterior Axis in Humans. *Current*
709 *Biology*, 28(13), 2129–2135.e6. <https://doi.org/10.1016/J.CUB.2018.05.016>
- 710 Chadwick, M. J., Bonnici, H. M., & Maguire, E. A. (2014). CA3 size predicts the precision of memory
711 recall. *Proceedings of the National Academy of Sciences of the United States of America*,
712 111(29), 10720–5. <https://doi.org/10.1073/pnas.1319641111>
- 713 Chen, J., Olsen, R. K., Preston, A. R., Glover, G. H., & Wagner, A. D. (2011). Associative retrieval
714 processes in the human medial temporal lobe: hippocampal retrieval success and CA1
715 mismatch detection. *Learning & Memory (Cold Spring Harbor, N.Y.)*, 18(8), 523–8.
716 <https://doi.org/10.1101/lm.2135211>
- 717 Collin, S. H. P., Milivojevic, B., & Doeller, C. F. (2015). Memory hierarchies map onto the hippocampal
718 long axis in humans. *Nature Neuroscience*, 18(11), 1562–1564. <https://doi.org/10.1038/nn.4138>
- 719 Dalton, M. A., Zeidman, P., Barry, D. N., Williams, E., & Maguire, E. A. (2017). Segmenting subregions
720 of the human hippocampus on structural magnetic resonance image scans: An illustrated
721 tutorial. *Brain and neuroscience advances*, 1, 2398212817701448.
- 722 Diedenhofen, B., & Musch, J. (2015). Cocor: A comprehensive solution for the statistical comparison
723 of correlations. *PLoS ONE*. <https://doi.org/10.1371/journal.pone.0121945>
- 724 Ding, S. L., & Van Hoesen, G. W. (2015). Organization and detailed parcellation of human
725 hippocampal head and body regions based on a combined analysis of cyto- and
726 chemoarchitecture. *Journal of Comparative Neurology*, 523(15), 2233–2253.
- 727 Dudukovic, N. M., Preston, A. R., Archie, J. J., Glover, G. H., & Wagner, A. D. (2011). High-resolution
728 fMRI reveals match enhancement and attentional modulation in the human medial temporal
729 lobe. *Journal of Cognitive Neuroscience*, 23(3), 670–82.
730 <https://doi.org/10.1162/jocn.2010.21509>
- 731 Fellini, L., Florian, C., Courtney, J., & Roullet, P. (2009). Pharmacological intervention of hippocampal
732 CA3 NMDA receptors impairs acquisition and long-term memory retrieval of spatial pattern
733 completion task. *Learning and Memory*, 16(6), 387–394. <https://doi.org/10.1101/lm.1433209>

- 734 Gold, A. E., & Kesner, R. P. (2005). The role of the CA3 subregion of the dorsal hippocampus in spatial
735 pattern completion in the rat. *Hippocampus*, *15*(6), 808–14.
736 <https://doi.org/10.1002/hipo.20103>
- 737 Gordon, A. M., Rissman, J., Kiani, R., & Wagner, A. D. (2014). Cortical Reinstatement Mediates the
738 Relationship Between Content-Specific Encoding Activity and Subsequent Recollection
739 Decisions. *Cerebral Cortex*, *24*(12), 3350–3364. <https://doi.org/10.1093/cercor/bht194>
- 740 Greve, D. N., & Fischl, B. (2009). Accurate and robust brain image alignment using boundary-based
741 registration. *NeuroImage*, *48*(1), 63–72. <https://doi.org/10.1016/j.neuroimage.2009.06.060>
- 742 Hindy, N. C., Ng, F. Y., & Turk-Browne, N. B. (2016). Linking pattern completion in the hippocampus to
743 predictive coding in visual cortex. *Nature Neuroscience*, *19*(5), 665–667.
744 <https://doi.org/10.1038/nn.4284>
- 745 Horner, A. J., Bisby, J. A., Bush, D., Lin, W.-J., & Burgess, N. (2015). Evidence for holistic episodic
746 recollection via hippocampal pattern completion. *Nature Communications*, *6*, 7462.
747 <https://doi.org/10.1038/ncomms8462>
- 748 Horner, A. J., & Burgess, N. (2013). The associative structure of memory for multi-element events.
749 *Journal of Experimental Psychology: General*, *142*(4), 1370–1383.
750 <https://doi.org/10.1037/a0033626>
- 751 Horner, A. J., & Burgess, N. (2014). Pattern completion in multielement event engrams. *Current*
752 *Biology : CB*, *24*(9), 988–92. <https://doi.org/10.1016/j.cub.2014.03.012>
- 753 Hunsaker, M. R., & Kesner, R. P. (2013). The operation of pattern separation and pattern completion
754 processes associated with different attributes or domains of memory. *Neuroscience &*
755 *Biobehavioral Reviews*, *37*(1), 36–58. <https://doi.org/10.1016/j.neubiorev.2012.09.014>
- 756 Jenkinson, M., Bannister, P., Brady, M., & Smith, S. (2002). Improved optimization for the robust and
757 accurate linear registration and motion correction of brain images. *NeuroImage*.
- 758 Jenkinson, M., & Smith, S. (2001). A global optimisation method for robust affine registration of brain
759 images. *Medical Image Analysis*. [https://doi.org/10.1016/S1361-8415\(01\)00036-6](https://doi.org/10.1016/S1361-8415(01)00036-6)

- 760 Johnstone, T., Ores Walsh, K. S., Greischar, L. L., Alexander, A. L., Fox, A. S., Davidson, R. J., & Oakes,
761 T. R. (2006). Motion correction and the use of motion covariates in multiple-subject fMRI
762 analysis. *Human Brain Mapping, 27*(10), 779–788. <https://doi.org/10.1002/hbm.20219>
- 763 Lee, H., Wang, C., Deshmukh, S. S., & Knierim, J. J. (2015). Neural Population Evidence of Functional
764 Heterogeneity along the CA3 Transverse Axis: Pattern Completion versus Pattern Separation.
765 *Neuron*. <https://doi.org/10.1016/j.neuron.2015.07.012>
- 766 Lee, I., & Kesner, R. P. (2004). Encoding versus retrieval of spatial memory: Double dissociation
767 between the dentate gyrus and the perforant path inputs into CA3 in the dorsal hippocampus.
768 *Hippocampus, 14*(1), 66–76. <https://doi.org/10.1002/hipo.10167>
- 769 Liang, J. C., & Preston, A. R. (2017). Medial temporal lobe reinstatement of content-specific details
770 predicts source memory. *Cortex, 91*. <https://doi.org/10.1016/j.cortex.2016.09.011>
- 771 Lisman, J. E. (1999). Relating Hippocampal Circuitry to Function: Recall of Memory Sequences by
772 Reciprocal Dentate–CA3 Interactions. *Neuron, 22*(2), 233–242. [https://doi.org/10.1016/S0896-6273\(00\)81085-5](https://doi.org/10.1016/S0896-6273(00)81085-5)
- 774 Maass, A., Berron, D., Libby, L., Ranganath, C., & Düzel, E. (2015). Functional subregions of the human
775 entorhinal cortex. *ELife, 4*, e06426. <https://doi.org/10.7554/eLife.06426>
- 776 McClelland, J. L., McNaughton, B. L., & O'Reilly, R. C. (1995). Why there are complementary learning
777 systems in the hippocampus and neocortex: Insights from the successes and failures of
778 connectionist models of learning and memory. *Psychological Review, 102*(3), 419–457.
779 <https://doi.org/10.1037/0033-295X.102.3.419>
- 780 Nakazawa, K., Quirk, M. C., Chitwood, R. A., Watanabe, M., Yeckel, M. F., Sun, L. D., ... Tonegawa, S.
781 (2002). Requirement for hippocampal CA3 NMDA receptors in associative memory recall.
782 *Science, 297*(5579), 211–218. <https://doi.org/10.1126/science.1071795>
- 783 Neunuebel, J. P., & Knierim, J. J. (2014). CA3 Retrieves Coherent Representations from Degraded
784 Input: Direct Evidence for CA3 Pattern Completion and Dentate Gyrus Pattern Separation.
785 *Neuron, 81*(2), 416–427. <https://doi.org/10.1016/j.neuron.2013.11.017>

- 786 Penny, W. D., Friston, K. J., Ashburner, J. T., Kiebel, S. J., & Nichols, T. E. (2011). *Statistical parametric*
787 *mapping: the analysis of functional brain images*. Elsevier.
- 788 Poppenk, J., Evensmoen, H. R., Moscovitch, M., & Nadel, L. (2013). Long-axis specialization of the
789 human hippocampus. *Trends in Cognitive Sciences*. <https://doi.org/10.1016/j.tics.2013.03.005>
- 790 Rosenthal, R., Rubin, D. B., & Meng, X.-L. (1992). Comparing correlated correlation coefficients.
791 *Psychological Bulletin*, *111*(1), 172–175. Retrieved from
792 <https://dash.harvard.edu/handle/1/11718225>
- 793 Schapiro, A. C., Kustner, L. V., & Turk-Browne, N. B. (2012). Shaping of object representations in the
794 human medial temporal lobe based on temporal regularities. *Current Biology : CB*, *22*(17),
795 1622–7. <https://doi.org/10.1016/j.cub.2012.06.056>
- 796 Staresina, B. P., Cooper, E., & Henson, R. N. (2013). Reversible information flow across the medial
797 temporal lobe: the hippocampus links cortical modules during memory retrieval. *The Journal of*
798 *Neuroscience : The Official Journal of the Society for Neuroscience*, *33*(35), 14184–92.
799 <https://doi.org/10.1523/JNEUROSCI.1987-13.2013>
- 800 Staresina, B. P., Henson, R. N. A., Kriegeskorte, N., & Alink, A. (2012). Episodic Reinstatement in the
801 Medial Temporal Lobe. *Journal of Neuroscience*, *32*(50), 18150–18156.
802 <https://doi.org/10.1523/JNEUROSCI.4156-12.2012>
- 803 Strange, B. A., Witter, M. P., Lein, E. S., & Moser, E. I. (2014). Functional organization of the
804 hippocampal longitudinal axis. *Nature Reviews Neuroscience*, *15*(10), 655–669.
805 <https://doi.org/10.1038/nrn3785>
- 806 Thakral, P. P., Wang, T. H., & Rugg, M. D. (2015). Cortical reinstatement and the confidence and
807 accuracy of source memory. *NeuroImage*, *109*, 118–129.
808 <https://doi.org/10.1016/j.neuroimage.2015.01.003>
- 809 Treves, A., & Rolls, E. T. (1991). What determines the capacity of autoassociative memories in the
810 brain? *Network: Computation in Neural Systems*, *2*(4), 371–397. <https://doi.org/10.1088/0954->
811 [898X_2_4_004](https://doi.org/10.1088/0954-898X_2_4_004)

- 812 Treves, A., & Rolls, E. T. (1994). Computational analysis of the role of the hippocampus in memory.
813 *Hippocampus*, 4(3), 374–391. <https://doi.org/10.1002/hipo.450040319>
- 814 Vazdarjanova, A., & Guzowski, J. F. (2004). Differences in hippocampal neuronal population
815 responses to modifications of an environmental context: evidence for distinct, yet
816 complementary, functions of CA3 and CA1 ensembles. *The Journal of Neuroscience : The Official*
817 *Journal of the Society for Neuroscience*, 24(29), 6489–96.
818 <https://doi.org/10.1523/JNEUROSCI.0350-04.2004>
- 819 Yushkevich, P. A., Piven, J., Hazlett, H. C., Smith, R. G., Ho, S., Gee, J. C., & Gerig, G. (2006). User-
820 guided 3D active contour segmentation of anatomical structures: Significantly improved
821 efficiency and reliability. *NeuroImage*, 31(3), 1116–1128.
822 <https://doi.org/10.1016/j.neuroimage.2006.01.015>
- 823 Zaitsev, M., Hennig, J., & Speck, O. (2004). Point spread function mapping with parallel imaging
824 techniques and high acceleration factors: Fast, robust, and flexible method for echo-planar
825 imaging distortion correction. *Magnetic Resonance in Medicine*, 52(5), 1156–1166.
826 <https://doi.org/10.1002/mrm.20261>
- 827 Zeidman, P., & Maguire, E. A. (2016). Anterior hippocampus: the anatomy of perception, imagination
828 and episodic memory. *Nature Reviews Neuroscience*, advance on.
829 <https://doi.org/10.1038/nrn.2015.24>
- 830
- 831

832 Figure Legends
833

834 *Figure 1.* Multi-element event paradigm (Horner et al., 2015). Participants learned 36 events that
835 consisted of multiple elements, with each element belonging to the location, people or object/animal
836 category. All events followed either a closed-loop structure [A] or an open-loop structure [B]. [C] At
837 encoding, events were learned in three blocks in a pairwise associative manner, one associative pair
838 at each block. [D] At retrieval, all three pairwise associations within each event were tested
839 bidirectionally. The 4-alternative forced choice recognition trial was followed by a confidence rating.
840

841 *Figure 2.* Example segmentation of hippocampal subfield dentate gyrus (DG, blue) and CA3 (yellow)
842 and coregistration from T2 to EPI space. The displayed images correspond to one participant. Manual
843 segmentation was performed on individual T2 images (Berron et al., 2017). Segmented masks were
844 then coregistered to the individual EPI space. Here, the coregistered masks are displayed on the
845 participant's mean EPI image, the lowest panel corresponds to the respective mean EPI. Crucial
846 hippocampal features for the segmentation (SLRM and the endfolial pathway on T2 images) are
847 indicated. Two corresponding slices in T2 and EPI space are shown from the hippocampal head (A)
848 and the hippocampal body (B). A sagittal view on the coregistration between an individual EPI and
849 the segmented hippocampal mask in T2 space (red outline) is presented in (C). EPI - echo-planar
850 image
851

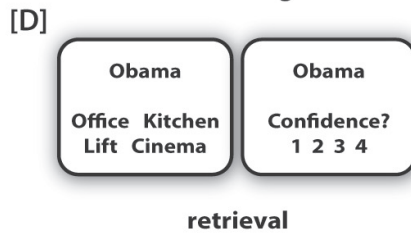
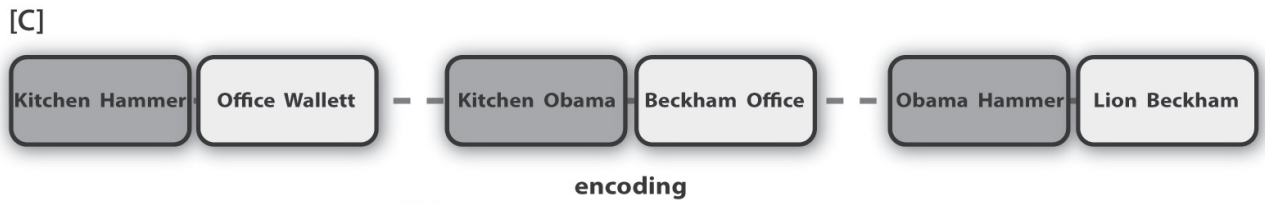
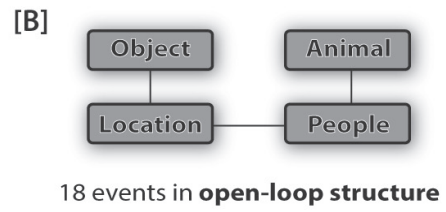
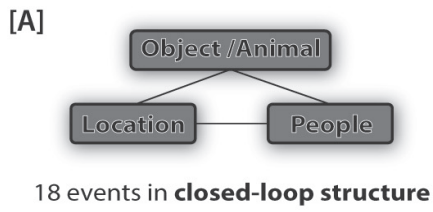
852 *Figure 3.* Overview “hippocampal activity – nontarget reinstatement” analysis procedure. [A]
853 Calculation of participant-specific nontarget reinstatement values. At each retrieval trial one event
854 element serves as a cue and one is the target. The additional element remains incidental to the task -
855 that is the nontarget (i). From the previous “element-specific activity at retrieval” analysis, cortical
856 clusters have been identified that specifically relate to the respective element categories (i.e. PHC for
857 location, MPC for people, LOC for object) (ii). For each participant, beta values are extracted from the
858 respective cluster for the condition that the category’s function at retrieval is to be a nontarget (iii).
859 Z-standardized beta values are averaged subsequently to obtain an overall nontarget reinstatement
860 value per participant. [B] Correlations between nontarget cortical reinstatement and hippocampal
861 activity. With a univariate first level GLM analysis, participant-specific contrast maps are obtained
862 that indicate the difference in hippocampal activity between the closed- and open-loop retrieval
863 condition. At group level that hippocampal activity pattern was correlated with the participant
864 specific nontarget reinstatement values. This yielded a statistical map, indicating hippocampal
865 activity at closed-loop retrieval that was scaled by the amount of nontarget reinstatement across
866 participants.
867

868 *Figure 4.* Behavioral dependency between multiple retrieval trials from closed- and open-loop
869 events. Observed dependency between trials from the same event was compared with estimated
870 dependency assuming fully independent and dependent models. Note that here depicted
871 dependency is calculated based on high confidence (level 3 – 4) versus collapsed low confidence
872 (level 1 – 2) and incorrect retrieval trials. Error bars ± 1 SE.
873

874 *Figure 5.* Difference in cortical reinstatement between element functions (i.e. cue, target, nontarget)
875 [A] across loop conditions (“overall” cortical reinstatement) and [B] subtracting cortical
876 reinstatement at open-loop from closed-loop retrieval. [A] *denotes significant difference ($p < .05$),
877 [B] *denotes significant difference from zero ($p < .05$)
878

879 *Figure 6.* Functional hippocampal activity correlations at closed-loop retrieval with overall nontarget
880 cortical reinstatement. [A] Hippocampal cluster whose difference in activity between retrieval of
881 closed- versus open-loop events correlates with amount of non-target reinstatement across
882 participants (cluster size $k = 35$; $p(\text{cluster}) = .028$ (uncorr)). [B] Correlations between cue, target and
883 nontarget cortical reinstatement and the extracted beta values for closed- versus open-loop
884 retrievals from the identified hippocampal cluster, respectively. * denotes significant differences
885 between correlations ($p < .05$).
886

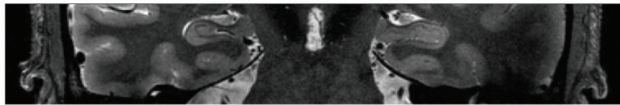
887 *Figure 7.* Functional activity correlations of subfield ROIs at closed-loop retrieval with overall
888 nontarget cortical reinstatement. Differences in activity between closed- and open-loop retrieval
889 were extracted as mean values from manually segmented hippocampal subfields CA3 and DG (right
890 anterior) and subsequently correlated with the amount of overall nontarget cortical reinstatement.



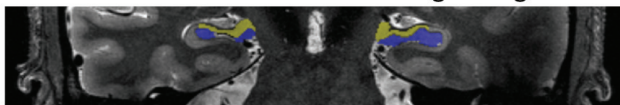
[A] hippocampal head

[B] hippocampal body

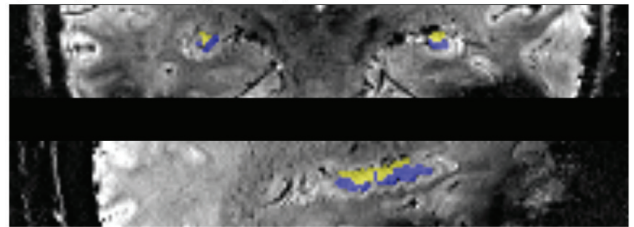
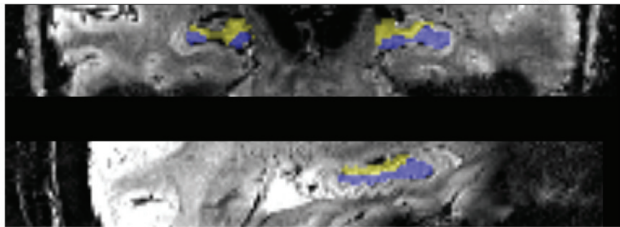
T2 image



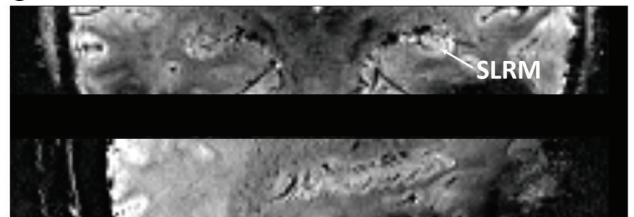
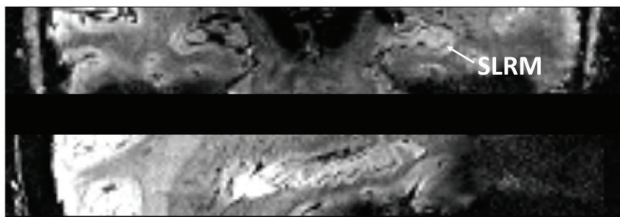
T2 image + segmented DG (blue) and CA3 (yellow)



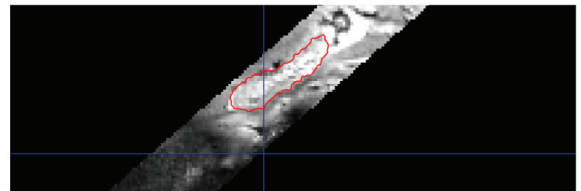
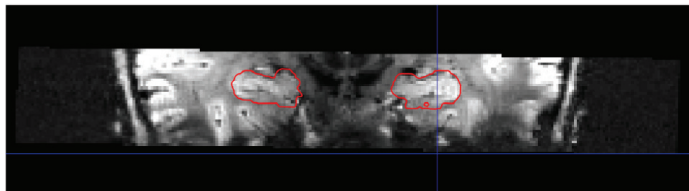
EPI image + coregistered DG (blue) and CA3 (yellow)

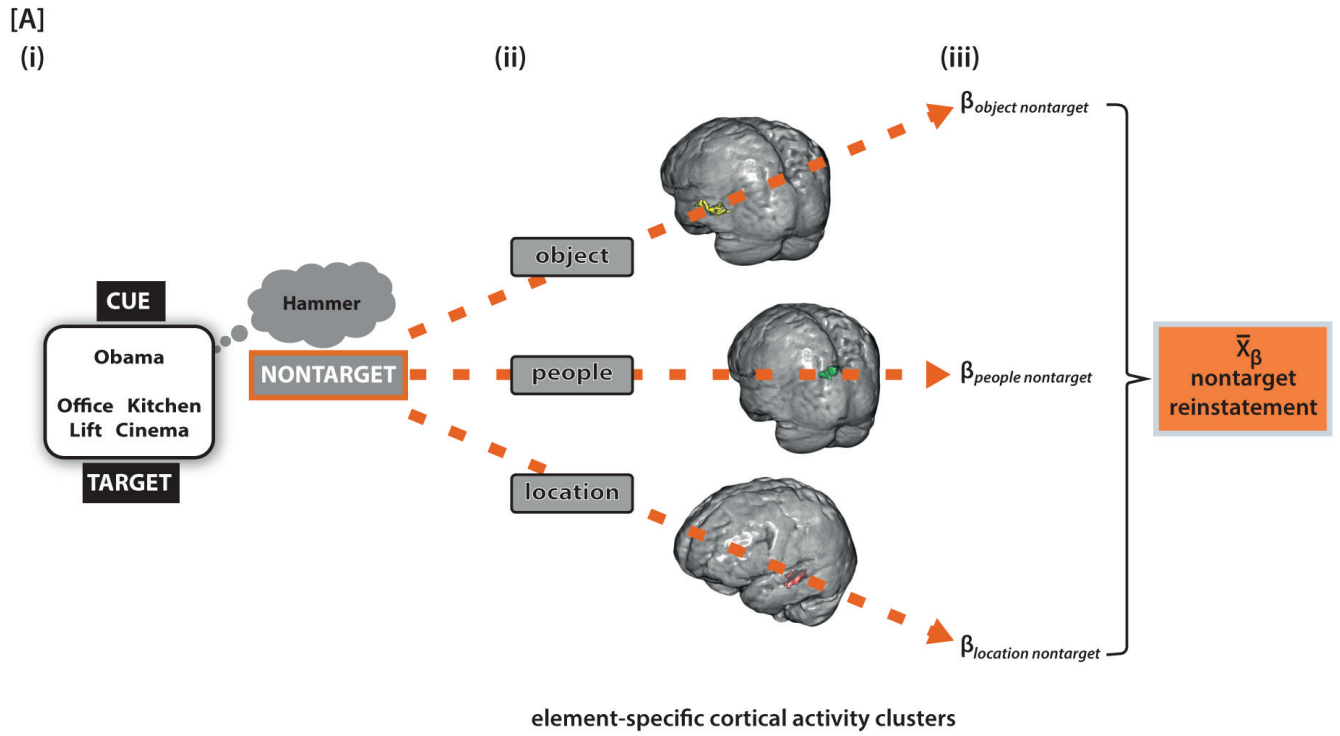


EPI image

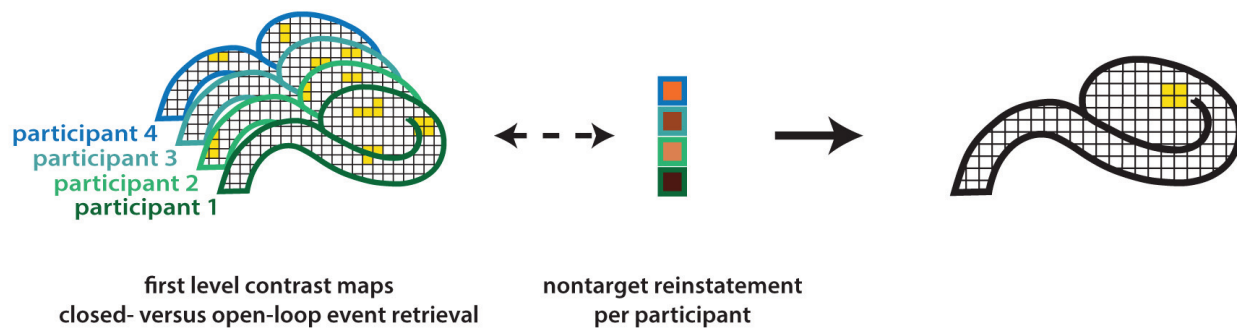


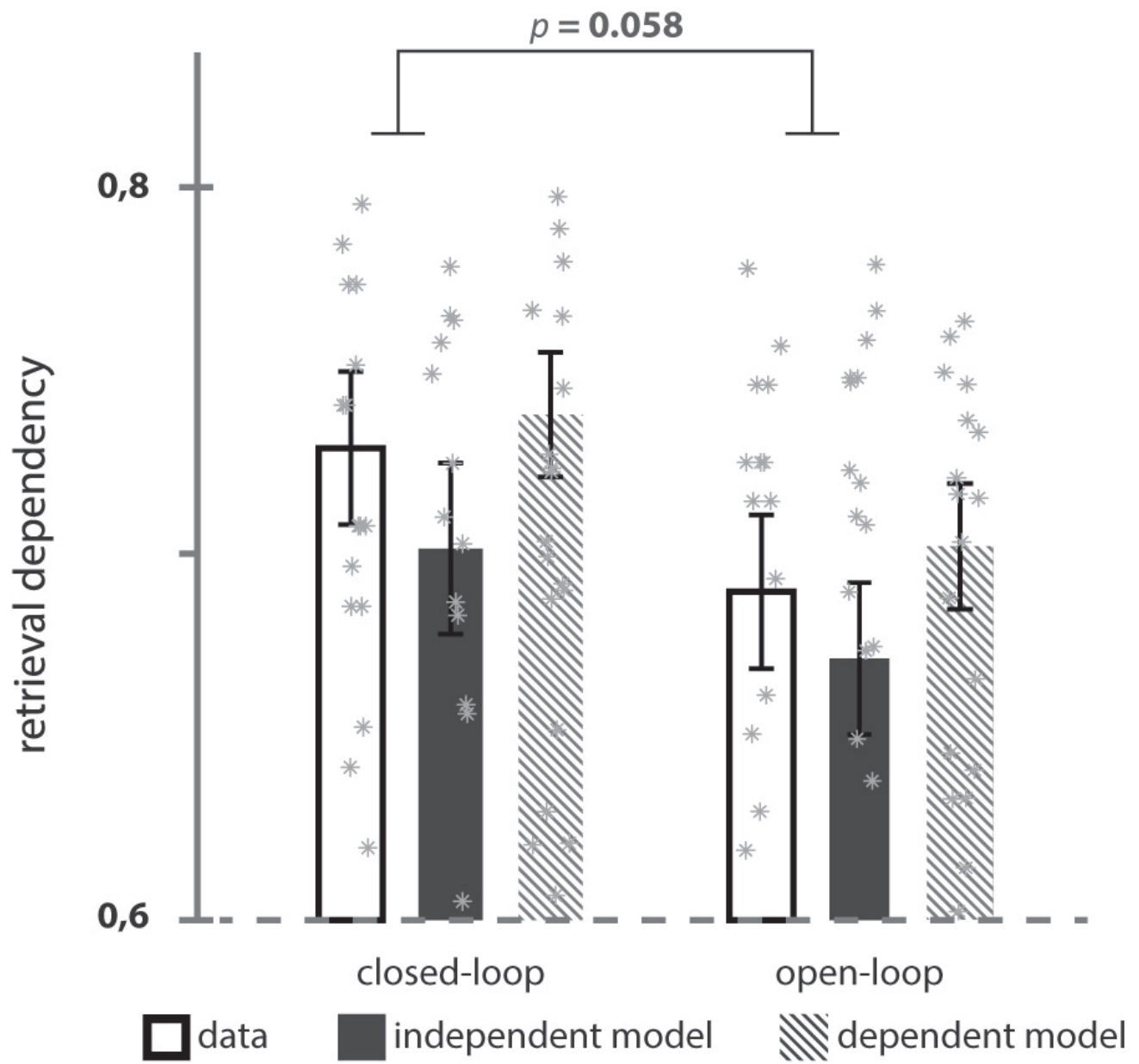
[C]



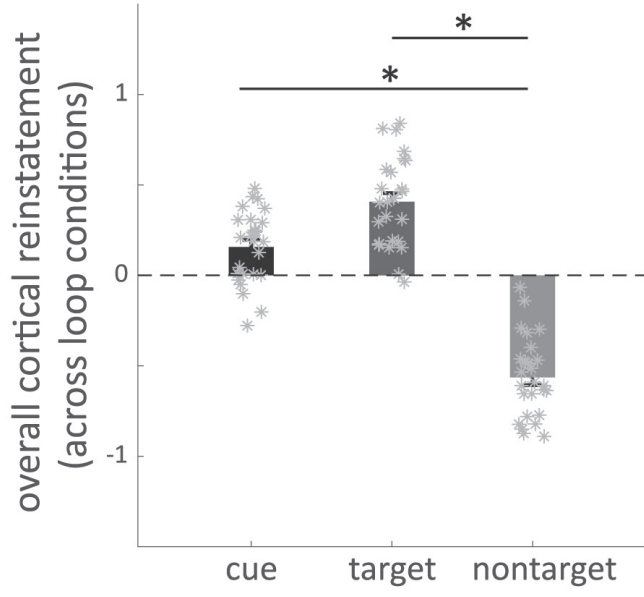


[B] correlation between nontarget reinstatement and hippocampal activity at closed loop event retrieval





[A]



[B]

